ORIGINAL PAPER

CrossMark

In-orbit performance of the LISA Pathfinder drag-free and attitude control system

A. Schleicher[1] · T. Ziegler[1] · R. Schubert[1] · N. Brandt[1] · P. Bergner[1] · U. Johann[1] · W. Fichter[2] · J. Grzymisch[3]

Abstract

LISA Pathfinder is a technology demonstrator mission that was funded by the European Space Agency and that was launched on December 3, 2015. LISA Pathfinder has been conducting experiments to demonstrate key technologies for the gravitational wave observatory LISA in its operational orbit at the L1 Lagrange point of the Earth–Sun system until final switch off on July 18, 2017. These key technologies include the inertial sensors, the optical metrology system, a set of μ-propulsion cold gas thrusters and in particular the high performance drag-free and attitude control system (DFACS) that controls the spacecraft in 15 degrees of freedom during its science phase. The main goal of the DFACS is to shield the two test masses inside the inertial sensors from all external disturbances to achieve a residual differential acceleration between the two test masses of less than 3×10^{-14} m/s^2/$\sqrt{\text{Hz}}$ over the frequency bandwidth of 1–30 mHz. This paper focuses on two important aspects of the DFACS that has been in use on LISA Pathfinder: the DFACS Accelerometer mode and the main DFACS Science mode. The Accelerometer mode is used to capture the test masses after release into free flight from the mechanical grabbing mechanism. The main DFACS Science Mode is used for the actual drag-free science operation. The DFACS control system has very strong interfaces with the LISA Technology Package payload which is a key aspect to master the design, development, and analysis of the DFACS. Linear as well as non-linear control methods are applied. The paper provides pre-flight predictions for the performance of both control modes and compares these predictions to the performance that is currently achieved in-orbit. Some results are also discussed for the mode transitions up to science mode, but the focus of the paper is on the Accelerometer mode performance and on the performance of the Science mode in steady state. Based on the achieved results, some lessons learnt are formulated to extend the results to the drag-free control system to be designed for future space-based gravity wave observatories like LISA.

Keywords LISA · LISA Pathfinder · DFACS · Drag-free control · In-orbit performance

1 Introduction

1.1 The LISA Pathfinder mission

LISA Pathfinder (LPF) [1] is a European Space Agency mission, implemented by Airbus, launched on December 3, 2015 and dedicated to an end-to-end experimental demonstration of the free fall of test masses (TMs) at the level required for a future space-based gravitational wave observatory, such as the laser interferometer space antenna (LISA) [2]. The test masses in LISA are the reference bodies at the ends of interferometer arms, and need to be free from spurious accelerations relative to their local inertial frame. Such accelerations would be in direct competition with the tidal deformations caused by gravitational waves. The LPF spacecraft houses two of the LISA test masses at the ends of a

✉ A. Schleicher
alexander.schleicher@airbus.com

1 Airbus, Claude-Dornier-Strasse 1, 88090 Immenstaad, Germany

2 Institut für Flugmechanik und Flugregelung, Universität Stuttgart, Pfaffenwaldring 27, 70569 Stuttgart, Germany

3 European Space Research and Technology Centre, Keplerlaan 1, Noordwijk, The Netherlands

Fig. 1 Unpacking of the LISA Pathfinder spacecraft after arrival at Europe's spaceport in Kourou, French Guiana. The propulsion module (left) and the science module (right) are shown

short interferometer arm, insensitive to gravitational waves, but sensitive to the differential acceleration between the test masses due to parasitic force effects which need to be carefully understood, controlled and budgeted during the design, implementation, and verification of LPF (see [3]). A photograph of the assembled LPF stack of the science module (right) including the scientific instrument and the propulsion module (left) for transfer to the target orbit around the L1 Lagrange point is shown in Fig. 1.

The main goal of the LISA Pathfinder mission is to verify that residual accelerations between its two test masses are below 3×10^{-14} m/s^2/$\sqrt{\text{Hz}}$ $[1 + (f/3 \text{ mHz})^2]$ in a Measurement Bandwidth (MBW) between 1 and 30 mHz. This is achieved with hardware and software algorithms that can be transferred to LISA which requires a single test mass acceleration noise below 3×10^{-15} m/s^2/$\sqrt{\text{Hz}}$ at 0.1 mHz. The acceleration noise requirement that was specified for LPF is relaxed by a factor of 10 compared to LISA and valid in a smaller frequency range to reduce the time and difficulty of ground testing. It was, however, considered sufficient to demonstrate that the technology can be transferred to LISA. This strategy has shown to be successful as discussed in [4] where the very first performances of LPF flight data are reported after the first 55 days of science operations. The system performed even better than expected and demonstrated functionality similar to a spacecraft needed as part of a LISA-like constellation to realize a space-based gravitational wave observatory.

1.2 The LISA technology package

The scientific instrument of LISA Pathfinder is called LISA technology package (LTP) and features the inertial sensor

subsystem (ISS), the optical metrology subsystem (OMS), the data and diagnostic subsystem (DDS) including a dedicated processing unit with interfaces to the on-board computer and other LTP equipment, and some auxiliary hardware like thermal shielding, gravity balance equipment, mechanical support structures, harness, and connectors. The ISS consists of two cubic test masses with surrounding electrode housings which are placed inside vacuum enclosures. The electrodes of the test mass housings allow the application of electrostatic forces and torques to the test masses and the measurement of all six degrees of freedom of each test mass by means of capacitive sensing techniques. The ISS also includes a caging and release mechanism to hold the test masses in place during launch and to slowly release them into free flight. In addition, the ISS houses hardware interfaces to inject ultraviolet light for contactless electrical test mass discharging, as well as heaters, thermometers, and magnetic coils to conduct disturbance experiments. Figure 2 shows a view of the LPF science module (left) and a zoom of important LTP hardware components (right) including the two vacuum enclosures with attached ultraviolet light feedthroughs and caging mechanisms, the test masses inside the electrode housings, and the optical bench as part of the OMS.

1.3 The drag-free control system

The drag-free and attitude control system (DFACS) of LISA Pathfinder is the control system for the science phase of the mission, controlling the spacecraft (SC) in 15 degrees of freedom. It has been developed by Airbus Defence and Space GmbH in Friedrichshafen (see [5, 6]). The degrees of freedom to be controlled include the 12 relative degrees of freedom of the two test masses as well as the attitude of the SC. The definition of the degrees of freedom is given in Fig. 3.

To control these degrees of freedom, the DFACS applies three different types of control loops:

- The drag-free control loop.
- The suspension control loop.
- The attitude control loop.

In the drag-free control loops, the SC is controlled with respect to the test masses in six degrees of freedom using either electrostatic measurements from the inertial sensor or optical measurements of the relative test mass coordinates and using the micro-propulsion system as the actuator. In the drag-free controlled degrees of freedom, the "SC follows the test mass" (see Fig. 4).

In the suspension control loops, the test masses are controlled with respect to the SC in the six non drag-free controlled degrees of freedom of the test masses. Again, the
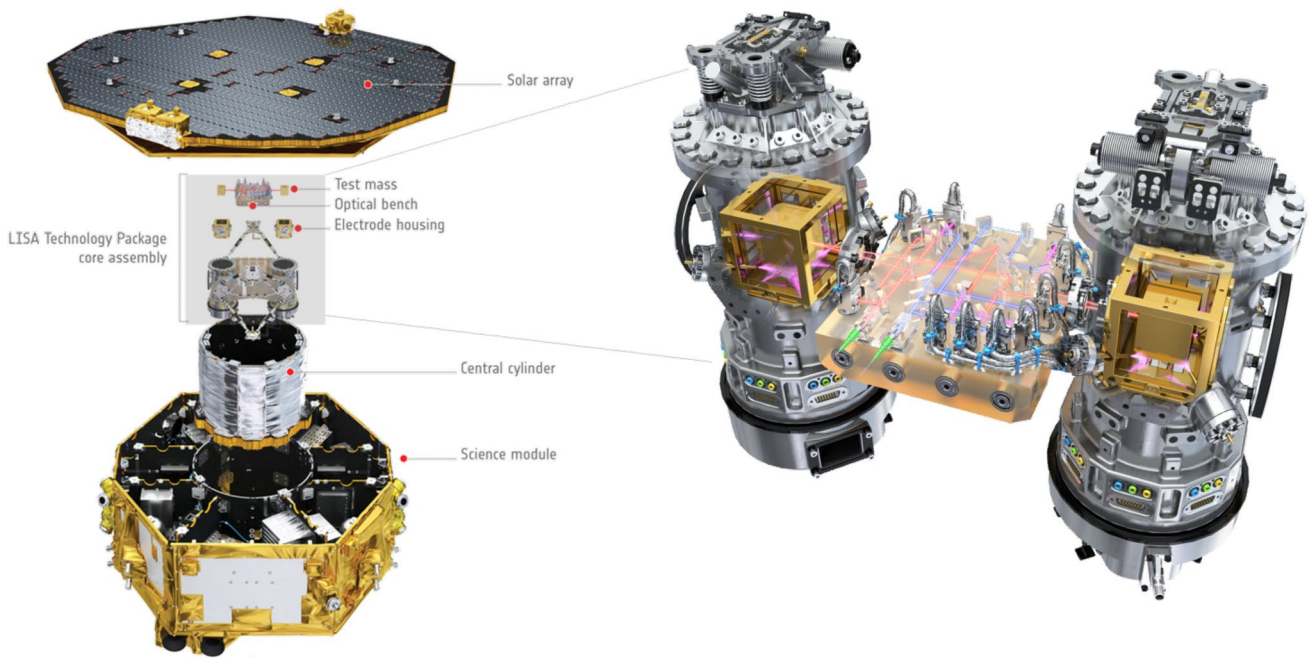
Fig. 2 Schematics of the LISA Technology Package (right) and its placement inside the LPF science module (left) with its μN cold gas thrusters

Fig. 3 Definition of the degrees of freedom relevant for LISA Pathfinder
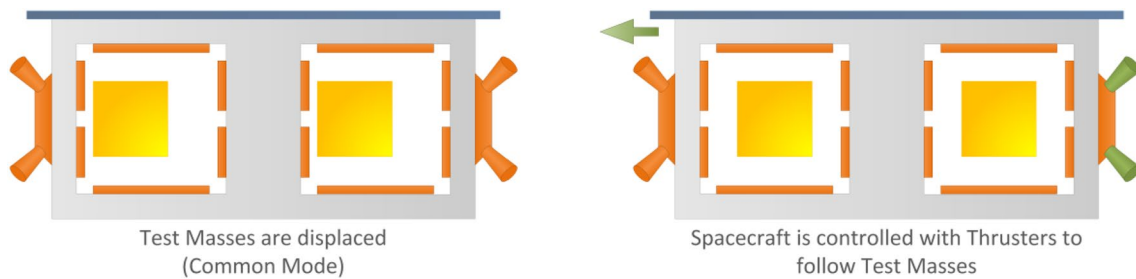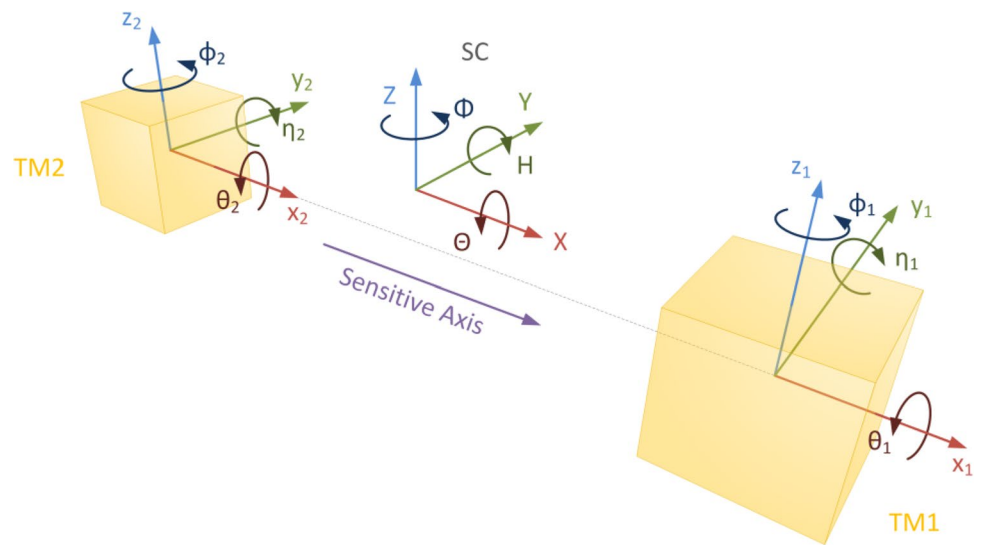

Fig. 4 The drag-free control principle

control loops use either electrostatic measurements from the inertial sensor or the measurements from the optical metrology system. The test masses are controlled using the electrostatic actuation capabilities of the inertial sensor. In the suspension controlled degrees of freedom the "test mass follows the SC" (see Fig. 5).

In the attitude control loop, the SC is controlled to follow a predefined reference attitude such that the SC is always pointing towards the sun and the antenna is always pointing towards the earth. These attitude control loops use the star trackers as sensors. Within the DFACS, attitude control is realized in two different ways. The direct attitude control is used in any mode without drag-free control. Here the attitude measurement from the star trackers and the reference attitude are used directly to control the three SC coordinates with thrusters (see Fig. 6).

The second type of attitude control is indirect and is used in any mode with drag-free control. Here the attitude is controlled by applying suspension control on some of the drag-free controlled axes (with the exception of the sensitive x-axis), thus forcing the SC to follow the test masses with the drag-free control loops. Using this scheme, it is possible to command the SC to follow the reference attitude, if the test masses are actuated accordingly, e.g., using suspension control to move both test masses in y (in opposite direction), the SC will be forced to rotate around its z-axis (see Fig. 7).
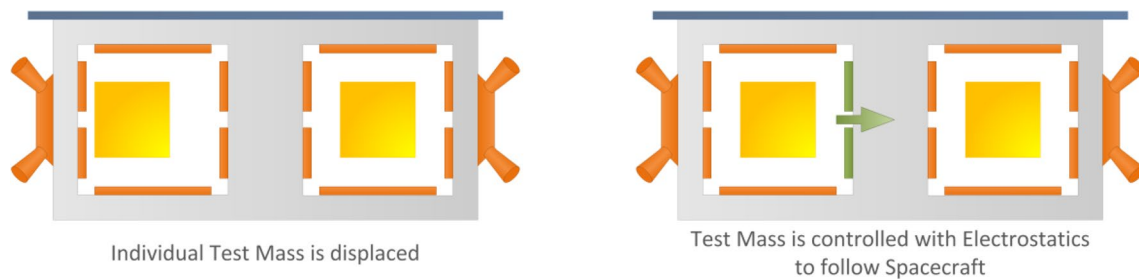

Individual Test Mass is displaced

Test Mass is controlled with Electrostatics to follow Spacecraft

Fig. 5 The suspension control principle

Initial Attitude Error

Spacecraft is controlled with Thrusters (Test Masses fully suspended)

Fig. 6 The direct attitude control principle

Test Masses are controlled with Electrostatics (deliberate Off-Pointing)

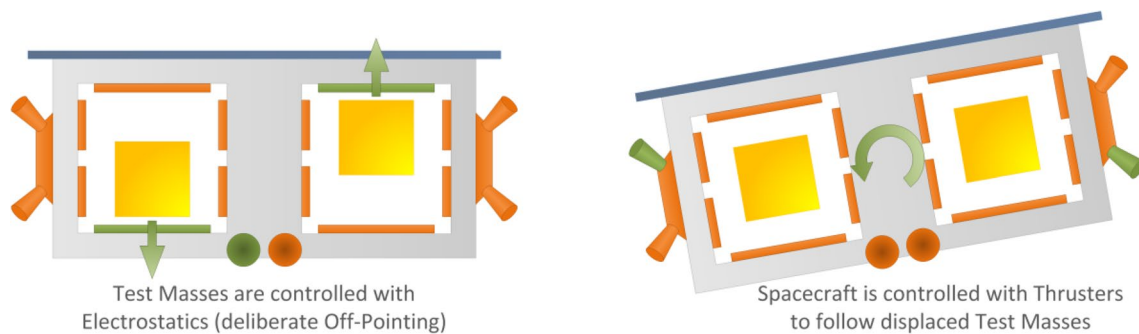Spacecraft is controlled with Thrusters to follow displaced Test Masses
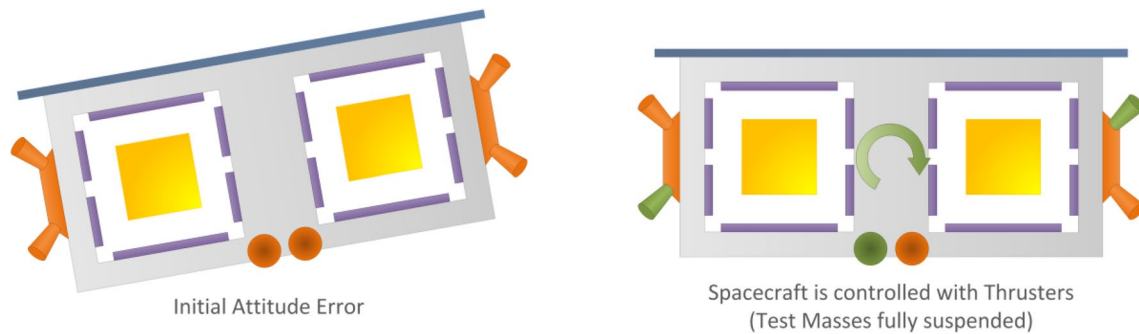
Fig. 7 The indirect attitude control principle

The different control loops are separated in bandwidth to minimize the cross-coupling between the loops. The drag-free loops have the highest bandwidths and the attitude control loops have the lowest bandwidths. For the design of the different loops, the highly coupled system has been decoupled through the definition of a decoupling matrix such that individual control loops can be designed as single–input–single–output (SISO) control loops. The controller outputs are then mapped back into forces and torques on the SC and the test masses via the decoupling matrix. The details of the decoupling scheme applied to LISA Pathfinder have been presented in [7].

The overall functional architecture of the DFACS is shown in Fig. 8. The main sensors for the DFACS are the two inertial sensors (IS), which provide electrostatic measurements for all 12 test mass degrees of freedom relative to the SC. In addition, the optical metrology system (OMS) provides optical measurements for six of the twelve test mass degrees of freedom (x_1, $x_2 - x_1$, $\eta_{1/2}$ and $\varphi_{1/2}$). Finally, the SC attitude is controlled using the two star trackers.

On the actuator side, the SC is controlled with a cold gas micro-propulsion system, which consists of a main and a redundant branch with six thrusters each. Note that all thrusters are canted towards the negative z-direction of the SC and can thus only provide thrust in the positive z-direction. As the SC is permanently oriented with the positive z direction towards the sun, the solar pressure is used as a virtual thruster to provide thrust in the negative z-direction. This minimizes the fuel consumption, but also limits the actuation authority that can be provided with the cold gas

system. This has been one of the biggest constraints for the design of the drag-free controllers and the mode transitions. The remaining degrees of freedom are controlled with the electrostatic actuation system provided by the ISS and which can control all 12 relative degrees of freedom of the two test masses. The electrostatic actuation system provides two different modes of operation, the wide range (WR) actuation mode and the high resolution (HR) actuation mode. The two modes link sensing and actuation, i.e., if actuation is switched to WR mode, so is the sensing. In WR mode, the actuation authority is much higher than in HR mode. At the same time, the noise on the measurements increases as well. Thus, WR mode is used mainly in accelerometer mode, where a large actuation authority is required to capture the test masses. On the other hand, HR mode provides a much small actuation authority, but at the same time also a much reduced sensing noise. Thus, HR actuation is applied during science modes, where the measurement accuracy is a key to meet the stringent performance requirements.

Due to the required functionality and the constraints from the hardware, a large number of modes had to be implemented for the DFACS. To minimize the number of modes, the DFACS application software (APSW) was implemented in a very modular way where modes can be defined via parameterization of the implemented modules. A limited number of baseline modes have been implemented in the APSW to ensure the basic functions are always available. In addition, two custom modes have been implemented that can be freely parameterized from ground to provide the
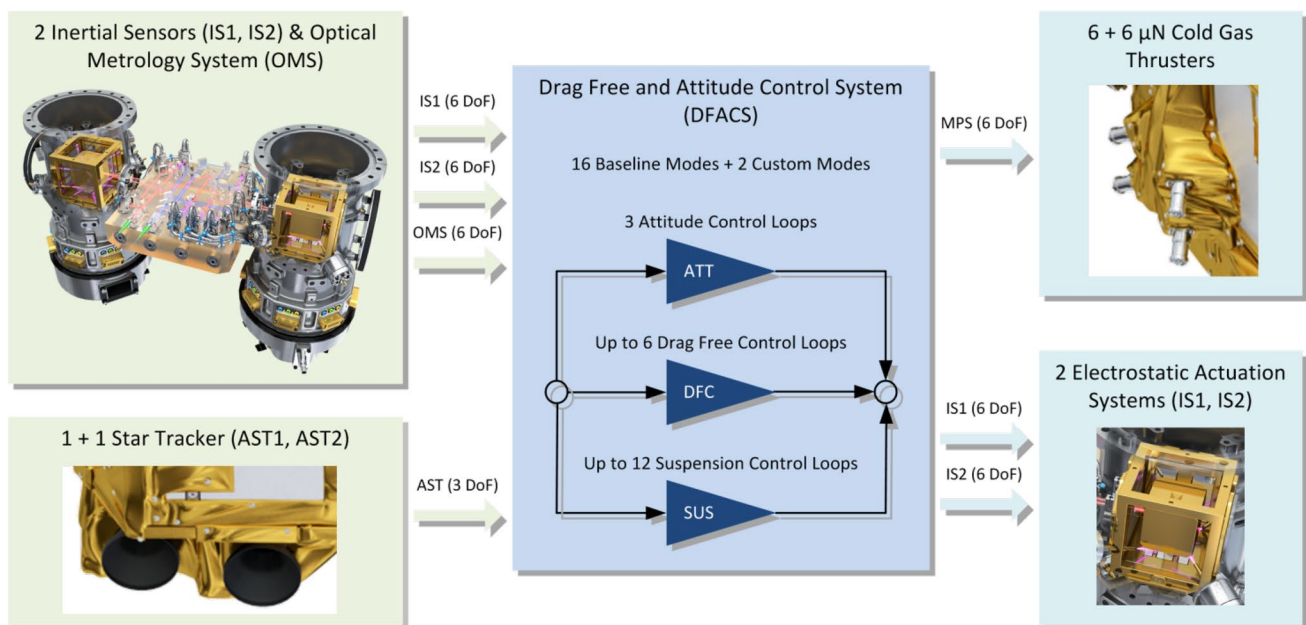

Fig. 8 DFACS functional architecture

necessary operational flexibility. The baseline modes can be grouped into three main categories

- Accelerometer modes (ACC)

    These modes all use direct attitude control and apply suspension control on all test mass degrees of freedom. A special type of accelerometer mode is the attitude mode (ATT), where both test masses are grabbed. The different submodes differ mainly in the test mass that is free (TM1, TM2 or both) and in the sensor signal used to control the test masses (ACC4 and ACC5 use optical measurements on some of the angular degrees of freedom). The accelerometer modes are also the modes that are used to capture the test masses after they have been released from the caging mechanism and to perform coarse TM discharging for LTP and DRS (NASA contribution) operation.

- Normal modes (NOM)

    These modes are the first modes that apply drag-free control on six of the 12 test mass degrees of freedom. Thus, the SC attitude is controlled using the indirect method. The normal modes are only intermediate modes that have been introduced to ensure a smoother transition from accelerometer mode to science mode.

- Science modes (SCI)

The science modes are the main experimental modes. The main science mode is science mode 1 (SCI1), which uses mostly optical measurements for control. The backup science mode is science mode 2 (SCI2), which uses only electrostatic measurements. Both science modes are separated into two submodes to provide a smooth transition to science conditions. A special experimental mode is the drift mode (DRIFT) where one or more of the test mass degrees of freedom are left floating freely with intermittent kicks being applied to move the test mass back into the center.

The configuration of the main mode types is summarized in Table 1.

This paper will focus on the performance in accelerometer mode, as it is used to capture the test mass during the critical release operation, and the performance in SCI1, as it is used for most of the scientific experiments on LISA Pathfinder.

Table 1 Mode configuration for the main mode types

Mode type	Attitude control scheme	Drag-free axes	Suspension axes	Test mass sensing	Test mass actuation
Attitude mode	Direct	Test masses grabbed		–	–
Accelerometer mode	Direct	–	All	Electrostatic or electrostatic + optical	WR
Normal mode	Indirect	$x_1, y_{1/2}, z_{1/2}, \theta_1$	$x_2, \theta_2, \eta_{1/2}, \varphi_{1/2}$	Electrostatic	WR or HR
Science mode	Indirect	$x_1, y_{1/2}, z_{1/2}, \theta_1$	$x_2, \theta_2, \eta_{1/2}, \varphi_{1/2}$	Electrostatic or electrostatic + optical	HR

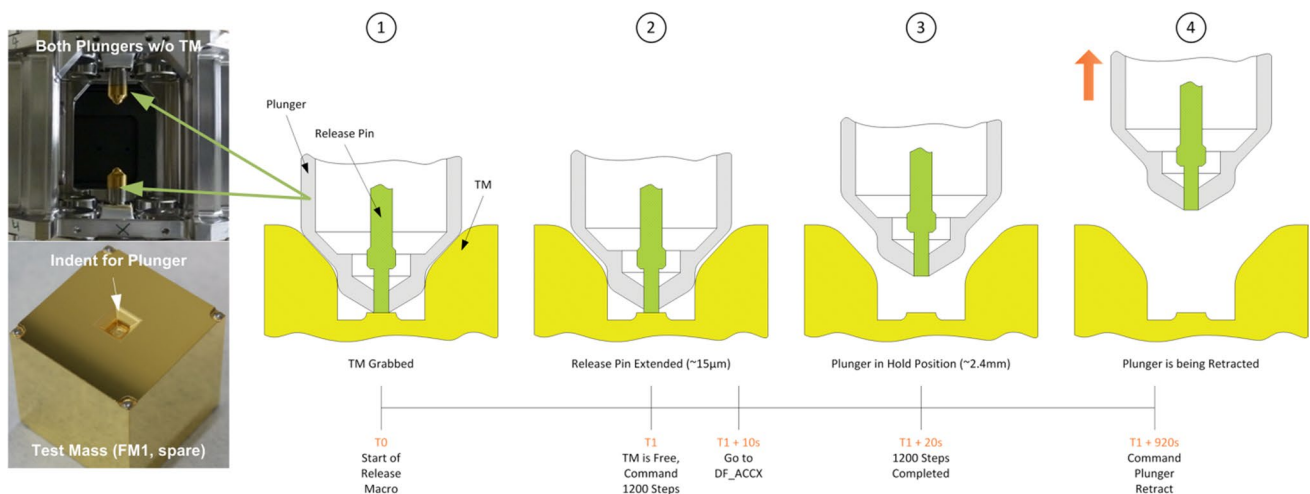**Fig. 9** Picture of EQM plungers and TM (left) and schematics of baseline TM release process (right)

2 Test mass release and accelerometer mode

2.1 Release process and requirements

The baseline test mass release process is shown in Fig. 9 from the state where the test mass is grabbed by the two plungers (only one plunger/TM interface is depicted) until the state where they are fully retracted. Full plunger retraction is done when the test masses are safely closed loop controlled in accelerometer mode. The release mechanism is designed to set the test masses into free flight with little initial displacement and velocity such that they can be captured by applying the available electrostatic forces and torques. The specified maximum test mass states after release are the initial conditions for the DFACS accelerometer mode and are summarized in Table 2.

As a baseline, test mass control in accelerometer mode is designed to start 10 s after the two release pins inside the plungers are synchronously pulled back by approximately 15 μm followed by an immediate and simultaneous retraction of the two plungers by more than 2 mm. This is illustrated in step (2) and (3) of Fig. 9.

This procedure is done to minimize electrostatic disturbances of the plungers on the test masses during closed loop control but still constraining the test mass motion in case of unexpected release conditions. The test masses are considered to be successfully captured as soon as the steady-state control requirements of Table 2 are met. The transition to the high performance drag-free control modes can be initiated afterwards.

Test mass capturing control is based on the non-linear sliding control methodology. This robust switching controller technique is used, because it applies maximum forces and torques and explicitly considers system non-linearities and model uncertainties (see [8]). Thus, it can cope with large initial offsets and velocities of the test masses after release without saturating the controller. These controllers have been implemented to improve the robustness of the release process, which is driven by the uncertainty in the release conditions.

Table 2 Requirements on initial test mass states after release from mechanism as well as steady-state control requirements for the case of using electrostatic readouts

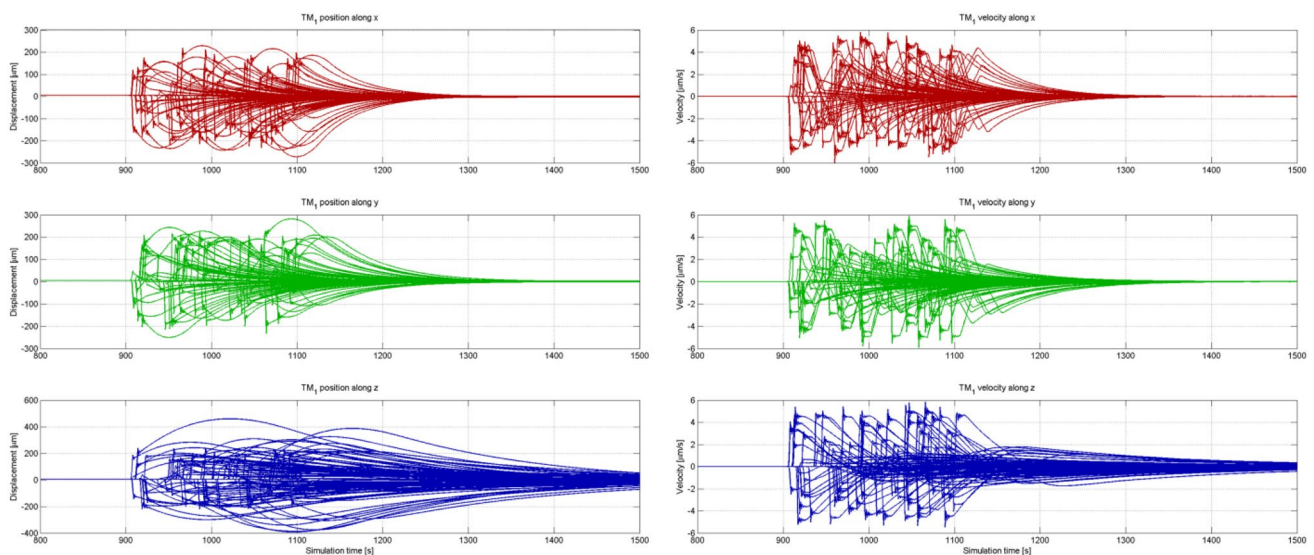| Test mass states	Requirements on initial TM state	Steady-state control accuracy (3σ)
Displacement w.r.t. TM housing	± 200 μm	< 25 μm
Attitude w.r.t. TM housing	± 2 mrad	< 100 μrad
Linear velocity, relative to TM housing	± 5 μm/s	< 1 μm/s
Rotational velocity, relative to TM housing	± 100 μrad/s	< 10 μrad/s

Fig. 10 First 100 Monte Carlo simulations predicting expected position and velocity of TM1 after release into free flight
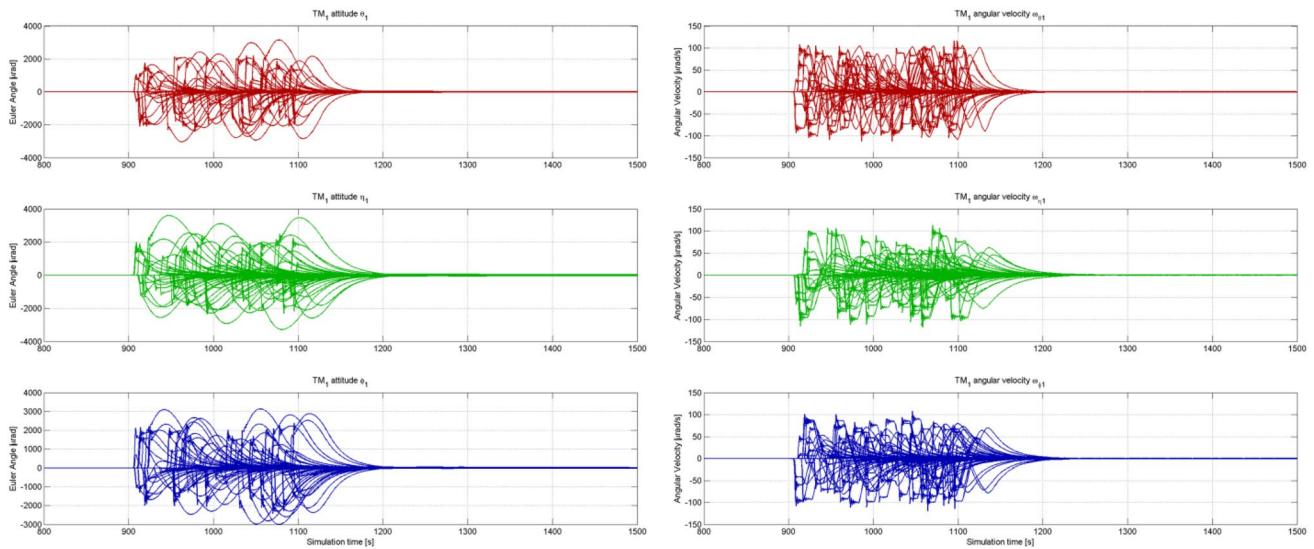
Fig. 11 First 100 Monte Carlo simulations predicting expected attitude and angular velocity of TM1 after release into free flight

2.2 On ground predictions

Verification of the test mass capturing control after release involves a large parameter space and is complex. A Monte Carlo simulation campaign has been set up to verify the accelerometer mode capability to cope with the required test mass release conditions. Each simulation run uses different values of the parameters defining the statistical ensemble. The first 100 release simulations are shown Figs. 10 and 11. From these test runs, one can see that the test mass displacements stay below 500 μm in translation and 4 mrad in rotation, which is well within the required envelope.

The verification campaign has been set up to run 2351 Monte Carlo simulation runs. At least 2329 runs would be needed to verify that the probability of a failure is less than 0.27% to a 95% verification confidence, assuming that two failures will be seen. All of the 2351 performed simulation runs met the previously defined success criteria when the test mass is released within the specified range applicable to the DFACS subsystem (see Table 2). Thus, for the simulated variation of the parameter space (test mass and spacecraft disturbances, initial conditions of test mass and spacecraft, etc.), the probability of a failure for a test mass release has been demonstrated to be less than 0.27% to a 95% verification confidence.

2.3 In-orbit performance

The first test mass release was initiated on February 15, 2016 with TM2. The release worked, but the overshoots seen during the release were much higher than expected from predictions. The position and attitude of TM2 during the release are shown in Fig. 12. The maximum overshoot in position was seen in the z-direction and was about
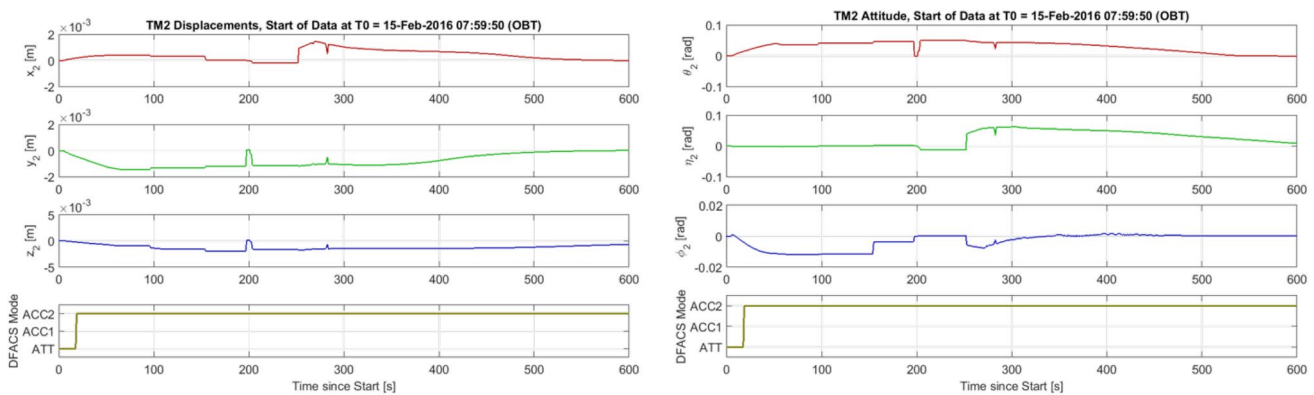

Fig. 12 TM2 position and attitude during first release on 15-Feb-2016

Table 3 Initial test mass state after release of TM2 compared to the release requirements of the release mechanism

Axis	Position/attitude	Requirement	Velocity/rate	Requirement
x_2	193.5 μm	± 200 μm	**7.5** μm/s	± 5 μm/s
y_2	**− 454.6** μm	± 200 μm	**− 22.3** μm/s	± 5 μm/s
z_2	**− 250.3** μm	± 200 μm	**− 16.4** μm/s	± 5 μm/s
θ_2	**15.4** mrad	± 2 mrad	**685** μrad/s	± 100 μrad/s
η_2	− 1.1 mrad	± 2 mrad	26.3 μrad/s	± 100 μrad/s
φ_2	**− 4.3** mrad	± 2 mrad	**− 250.7** μrad/s	± 100 μrad/s

Bold values are the ones that have violated the requirement

2 mm. The maximum overshoot in rotation was seen in θ and was about 50 mrad. From the time series in Fig. 12, periods of constant test mass motion can be seen. In these areas, the low level sensing FDIR was triggered as the test mass actually left the sensing range of the inertial sensor. Analyses performed later have shown that the test mass actually hit the plunger at one point. The root cause for the issues was the initial release velocity of the test mass. Analyses of the test mass motion and the estimated test mass velocities and rates have shown the initial velocities after release were far beyond anything considered on ground. The estimated initial conditions at release are summarized in Table 3.

Nevertheless, even under these conditions, the DFACS was able to capture the test mass and control it to steady state. This has been made possible by the sliding mode implementation of the accelerometer mode controllers, which is designed specifically to cope with large initial offsets and velocities.

The next release was performed on February 16, 2016 for TM1. A similar situation was observed where again the initial test mass states after release were far beyond the requirements the DFACS has been designed for. Nevertheless, with some additional update of the release process, the test mass could again be captured by the DFACS and controlled safely to steady state.

Following the initial release, the test masses have been captured and released a couple of times with similar initial conditions for the control. Nevertheless, the DFACS has always been able to capture the test masses and bring the SC back into science mode.

3 Transition to science mode

3.1 Mode transitions and constraints

The transition to science mode is initiated once both test masses have been captured successfully and steady state has been reached in accelerometer mode. The nominal transition sequence between accelerometer mode and science mode is shown in Fig. 13 together with the minimum wait durations in between mode transitions that have been derived before launch.

During commissioning, the first transitions have been commanded from ground during contact. Once the first in-orbit verification was completed, the wait durations have been adjusted gradually to minimize the transition duration to science mode. In the meantime, mode transitions to science mode are commanded regularly outside of ground contact.

The main constraints for the mode transition are the actuation authorities of the micro-propulsion system and the electrostatic actuation system. The critical transitions are the ones from ACC3 to NOM1 and from NOM1 to NOM2. The first transition is critical, as the control scheme is changed from pure suspension control to a mixture of drag-free and suspension control. In addition, the control is switched from nonlinear sliding mode controllers to linear controllers. This can cause larger transients that may cause saturation in the controllers. The second transition is critical, as the suspension control is switched from WR to HR actuation, which means a change in actuation authority. To ensure a smoother transition between the modes, the DFACS has implemented two measures. On one side, a controller initialization scheme has been implemented that ensures that
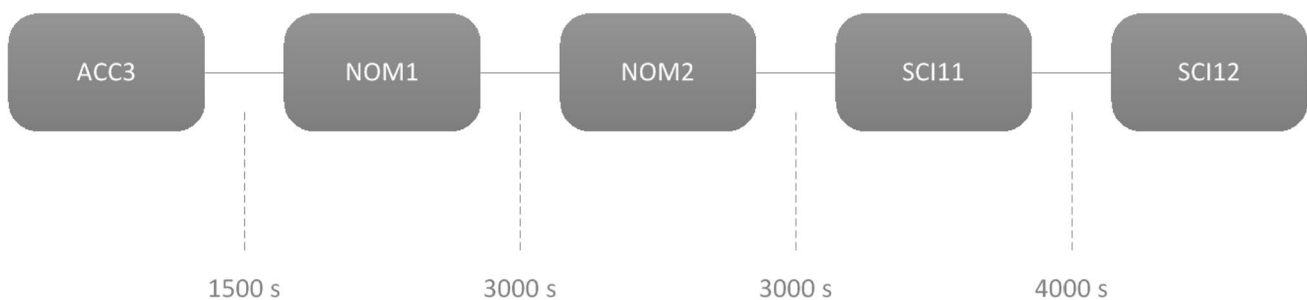

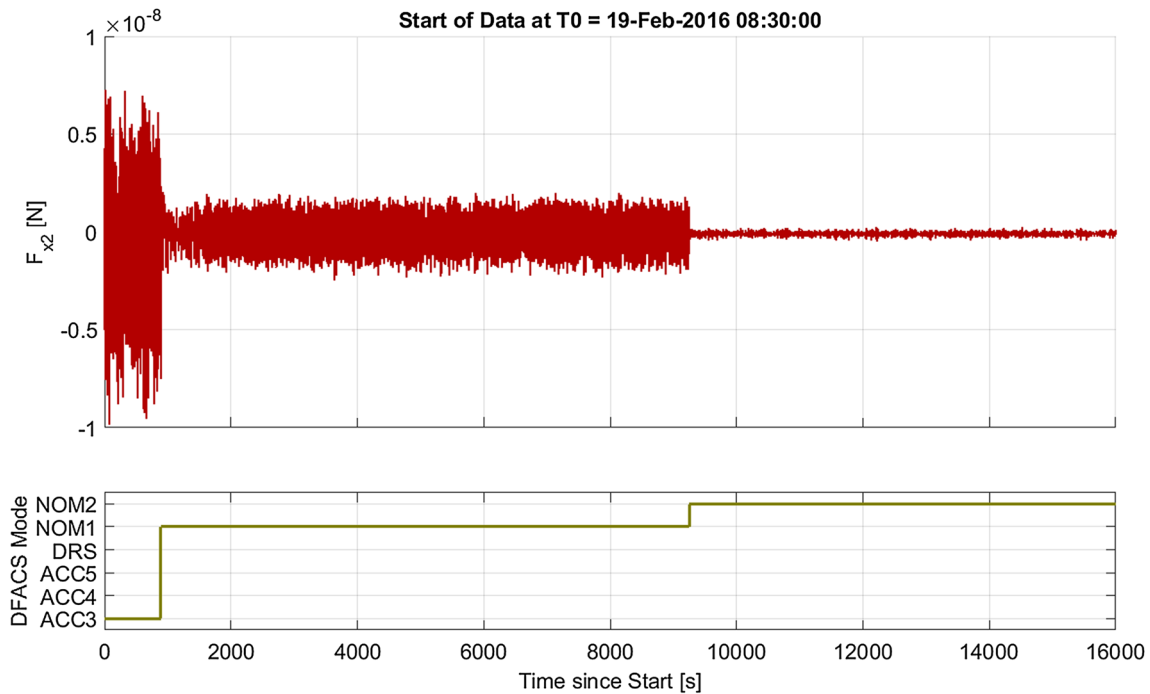**Fig. 13** Transition from accelerometer mode (ACC3) to science mode 1 (SCI12)

Fig. 14 Commanded force on x_2 during the first transition from ACC3 to NOM2 on 19-Feb-2016
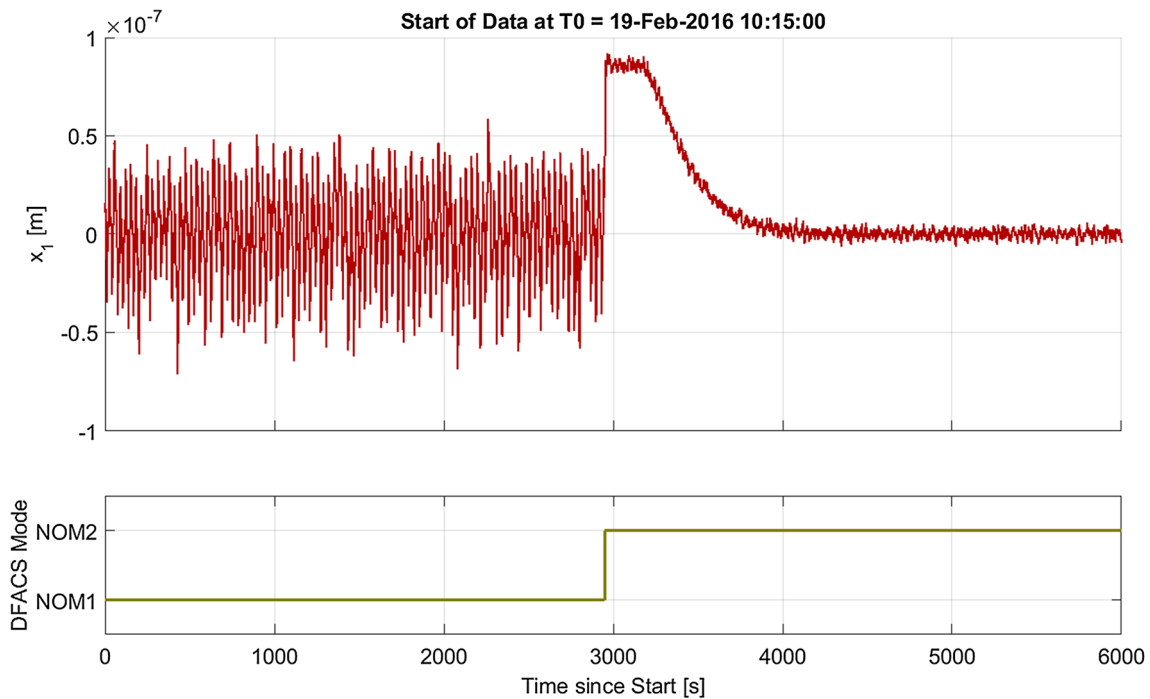

Fig. 15 Measured position of x_1 during first transition from NOM1 to NOM2 on 19-Feb-2016

the controller output does not introduce any jumps on the system. Figure 14 shows an example of the result of the controller initialization scheme. The plot shows the commanded

force for the electrostatic actuation system on TM2 in x for the first transitions from ACC3 to NOM1 and from NOM1 to NOM2 during commissioning. No transients are seen on

the commanded force, as the controller initialization scheme forces the controller output to stay at the same level during the mode transition.

On the other hand, so-called slew maneuvers have been implemented. These slew maneuvers ensure that any jumps on the controller inputs are not fed into the controller directly, but are driven to zero on a trajectory that is derived based on predefined constraints like the maximum velocity and maximum acceleration. An example for the slew maneuver is shown in Fig. 15 for the position of TM1 in x as measured by the inertial sensor. The plot shows again the first transition from NOM1 to NOM2 during commissioning. The jump in the measurement that is seen at the instance of mode transition is a result of the difference in calibration error between WR and HR electrostatic measurements. However, due to the slew functionality, this jump is not transmitted to the controller input. Instead, a trajectory is defined that drives the measurement error to zero in a smooth manner. Slew maneuvers are applied every time a mode transition switches between sensor signals or controllers and if steady state has not been reached in the previous mode.

3.2 In-orbit performance

Over the course of the mission, the system has been switching back and forth between accelerometer mode and science modes on a regular basis, since regular station keeping is required to correct the drift of the SC in L1. These station keeping maneuvers are performed in ACC3. The transition to science mode has proven to be very stable and repeatable. As an example, the position of TM1 and the attitude of TM1 are shown in Fig. 16 for multiple mode transitions
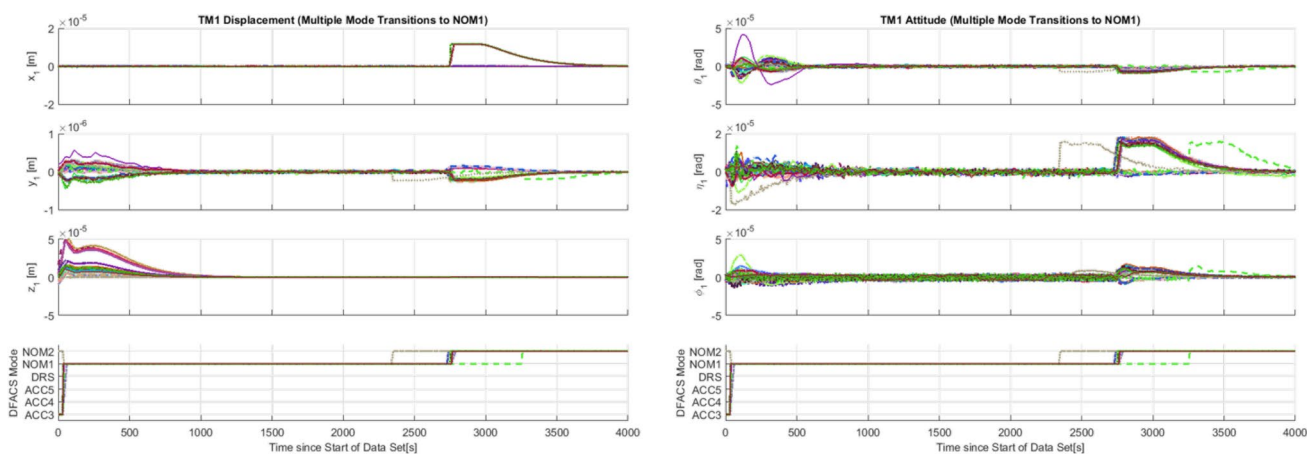

Fig. 16 Position (left) and attitude (right) of TM1 during transition from ACC3 to NOM1 and NOM2 for mode transitions between March 2016 and February 2017
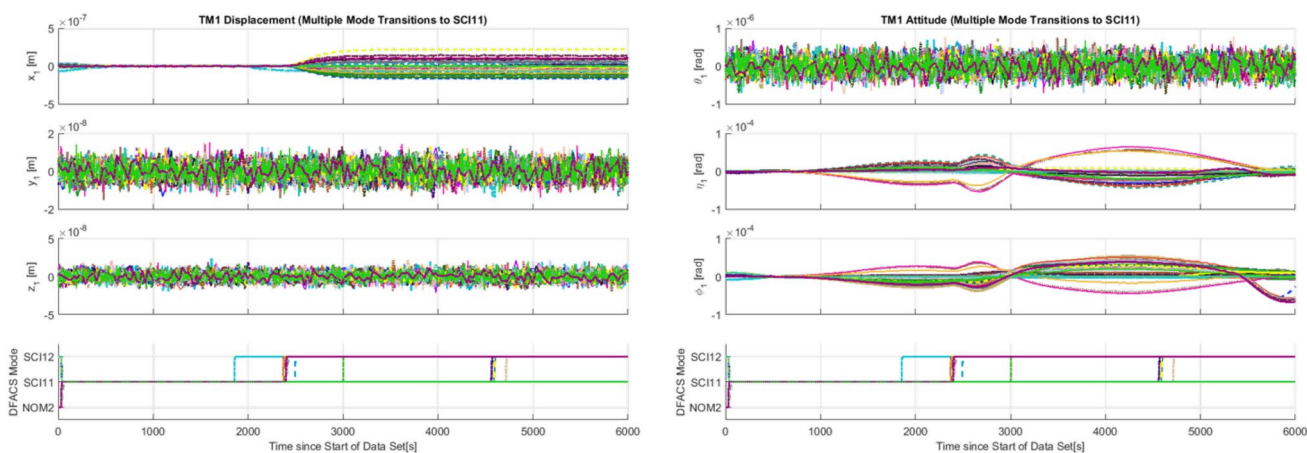

Fig. 17 Position (left) and attitude (right) of TM1 during transition from NOM2 to SCI11 and SCI12 for mode transitions between March 2016 and February 2017

to NOM1 and then to NOM2 in the period from March 2016 to February 2017.

The transitions to SCI11 and then to SCI12 for multiple mode transitions are shown in Fig. 17 for the same period. In both cases, the repeatability of the mode transitions is exceptional and in line with expectations from ground predictions. Thus, the mission so far has shown that the transition to science mode is very stable.

4 Science mode

4.1 Requirements

The main performance index for the science performance of LISA Pathfinder is the differential acceleration between the two test masses in the x-axis, which is also referred to as the sensitive axis. For LISA Pathfinder, the requirement states that the differential acceleration in the sensitive axis reconstructed from the optical measurement of the differential position $\Delta x = x_2 - x_1$ shall meet the following condition:

$$\mathrm{RPSD}_{\Delta \ddot{x}} \leq 3.0 \times 10^{-14} \times$$
$$\left(1 + \left(\frac{f}{3\mathrm{mHz}}\right)^2\right)\left[\frac{\mathrm{m/s^2}}{\sqrt{\mathrm{Hz}}}\right] \quad \text{for} \quad 1\mathrm{mHz} \leq f \leq 30\mathrm{mHz}.$$

The requirement specified in Eq. (1) is a requirement in the frequency domain on the root power spectral density (RPSD) of the differential test mass acceleration and is valid in the MBW. Note that the requirement is valid for science mode 1. A less stringent requirement is applicable for science mode 2. However, this paper will focus on the main science mode, as science mode 2 has not been used during the science phase and was only verified once during commissioning. The requirement is actually one order of magnitude more relaxed than the requirement for LISA, which is also applicable for a wider frequency band. Nevertheless, even the LISA Pathfinder requirement is already orders of magnitude more stringent than any previous or current drag-free mission.

The measurement equation for the optical measurement of the differential position in the sensitive axis is described by the following equation:

$$\Delta x_{\mathrm{OMS}} = \mathrm{SG}_{x_2} \times \left(\underbrace{f_{x_2} - f_{x_1}}_{\Delta f_x} - \underbrace{\left(\omega_{x_2}^2 - \omega_{x_1}^2\right)}_{\Delta \omega_x} \times x_1\right) + S_{x_2} \times \eta_{\mathrm{OMS}}.$$
$$(2)$$

The elements of the measurement equation specified in Eq. (2) are the following:

SG_{x_2} Disturbance reduction transfer function of the x_2 control loop.

Δf_x Differential forces acting on the test masses in x, including direct forces on the test masses, non-gravitational forces acting on the SC as well as crosstalk from the other axes.

$\Delta \omega_x$ Differential "stiffness" in x, i.e., the sum of all force gradients that scale with the offset of the test masses in x (gravity gradient, sensing errors, actuation errors, etc.).

x_1 The offset of TM1 in x relative to the housing/SC.

S_{x_2} The sensitivity function of the x_2 control loop.

η_{OMS} The measurement noise of the optical differential position measurement in x.

To recover the differential acceleration from the optical measurement of the differential position, the measurement signal is multiplied with the inverse of the disturbance reduction of the x_2 control loop that has been estimated on ground:

$$\Delta \ddot{x} = \mathrm{SG}_{x_2}^{-1} \times \Delta x_{\mathrm{OMS}}. \tag{3}$$

It can be seen from the measurement equation that the science performance is driven on one side by the hardware performance and in particular by the accuracy of the OMS and on the other side by the performance of the DFACS itself and its ability to suppress disturbances and crosstalk.

When looking at the predicted performance prior to launch in Fig. 18, it can be seen that the performance in the MBW is actually driven by the noise of the electrostatic actuation system (from the x_2 actuation), which cannot be influenced by the control loop. The second main contributor is the differential TM disturbance noise (mainly self-gravity). At higher frequencies, the OMS readout noise becomes the driver. Below the MBW, the star tracker noise (AST) becomes the driver around the frequency that coincides with the bandwidth of the attitude controllers (around 2×10^{-4} Hz). This contribution is the influence of the SC attitude motion on the test masses that enters via crosstalk from the attitude control loops. The contribution from the micro-propulsion system (MPS) enters directly via the control performance in x_1 and via crosstalk from the other drag-free controlled axes. The inertial sensor readout (IS) enters also via crosstalk from the other axes. When looking at the different contributions, it can be seen that the DFACS has been designed such that the performance is limited by the hardware constraints and not by the performance of the control system.

The main performance index has been broken down further to the level of individual control axes, e.g., test mass motion that would enter via the "stiffness" in the system
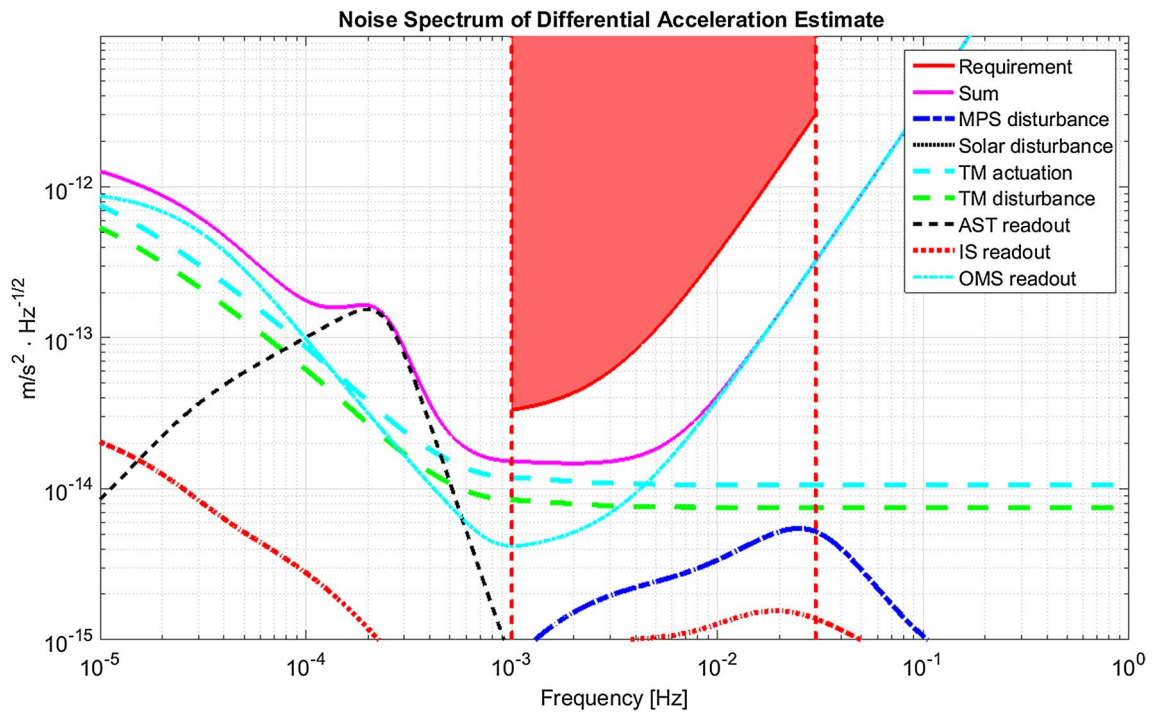
Fig. 18 Predicted differential acceleration performance prior to launch
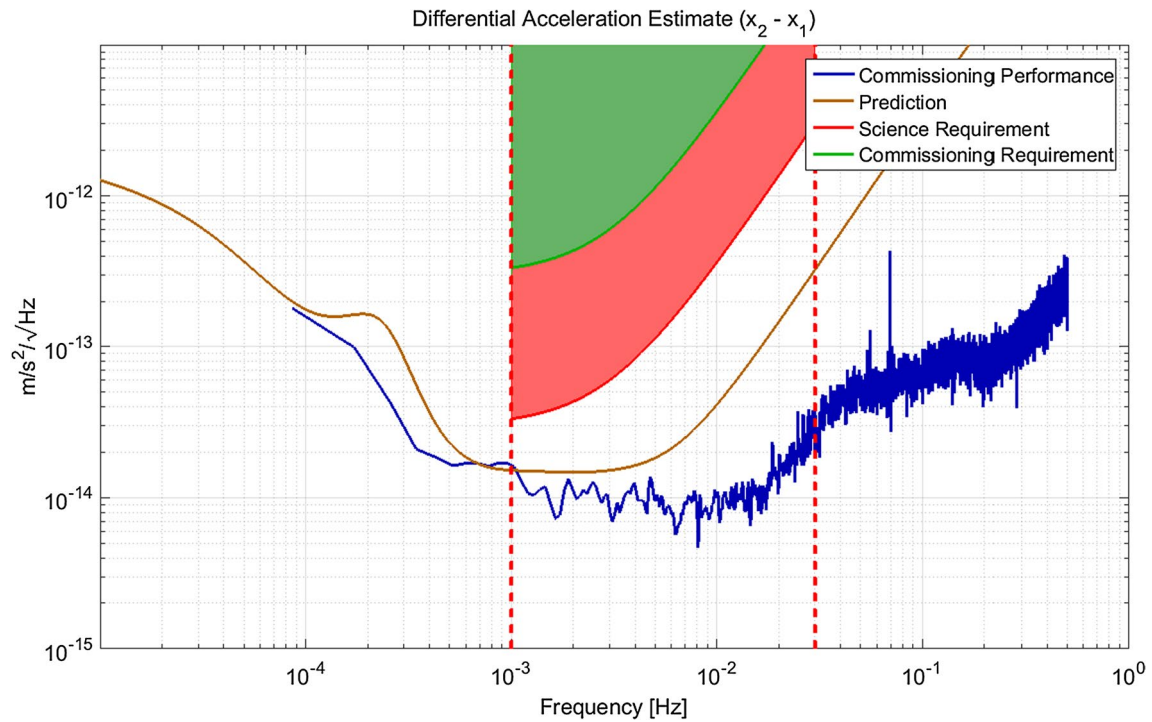

Fig. 19 Differential acceleration in SCI12 during commissioning

or commanded forces and torques that would enter via the actuation crosstalk in the electrostatic actuation system. However, this paper will focus on the main performance index, as it is a clear indicator for the overall performance of the (highly coupled) system.

4.2 In-orbit performance

The first verification of the differential acceleration performance was achieved during commissioning. For the in-orbit verification, a dedicated requirement was established that was one order of magnitude less stringent than the science requirement, i.e., 3.0×10^{-13} m/s^2/$\sqrt{\text{Hz}}$ instead of 3.0×10^{-14} m/s^2/$\sqrt{\text{Hz}}$. Science mode 1 (SCI12) was entered for the first time on February 23rd 2016. For the derivation of the differential acceleration, a data segment of about 60,000 s was used. The result of the derivation is shown in Fig. 19 together with the predicted performance prior to launch as well as the science and the commissioning requirement. The performance shown is reconstructed directly from the optical measurement of the differential position by multiplying the measurement with $SG_{x_2}^{-1}$. No additional post-processing has been performed on the data. The plot shows that even the first raw performance estimate meets not only the commissioning requirement, but already the science requirement of the LISA Pathfinder mission. In addition, the performance is even better than predicted prior to launch. The main reason for the better performance in-orbit is the hardware performance and in particular the OMS performance. The readout noise of the OMS is much lower in-orbit than predicted on ground. In addition, also the noise from the electrostatic actuation system and the differential TM disturbance noise are lower than predicted. It was shown by the science team in [1] that the bump that is evident between 20 and 200 mHz is the pickup of the SC motion by the optical measurement of the differential test mass position, which can be reduced by improving the beam alignment in the OMS through defined rotations of the test masses. Any residual contribution can then be removed in post-processing.

Since commissioning, the performance has been improved even further, as more and more contributors have been characterized by the science team. These characterizations have enabled the science team to improve their post-processing of the data. In addition, the system has been improved by optimizing the optical readout, by the gradual decrease of the residual gas pressure in the inertial sensors and by modifying the parameterization of the electrostatic actuation algorithm in the DFACS to reduce the actuation authority and thus also the noise level. The latter modification is only possible due to the flexible and modular implementation of the DFACS APSW. However, the modification can only be applied once in steady state, since the residual actuation authority is too small for the mode transitions. All these modifications have improved the performance almost to the level of the more stringent LISA requirement. More information on the latest science performance can be found in [4, 9].

5 Mode statistics

Between the first start of the DFACS during commissioning in February 2016 and the last in-orbit performance review beginning of March 2017, the DFACS has been used extensively for scientific experiments, applying the full range of modes available, including the custom modes. In this period, the DFACS has spent a total of 164 days in science mode 1 (SCI1) where most of the experiments have been performed. A total of 72 days have been spent in accelerometer mode 3, which is the DFACS safe mode. It is used as a first fallback in case of anomalies and is also used regularly for station keeping. Another 62 days have been spent overall in accelerometer mode 5, which uses optical measurements on some of the rotational degrees of freedom. It has been used mainly of OMS calibration activities and discharging of the test masses. The last major contributor is the drag reduction system (DRS) mode. This is a special mode, where the American control system is in control of the SC to perform its own experiments. Nevertheless, even in DRS mode, the DFACS provides the test mass position and attitude measurements to the DRS and converts the force and torque commands for the electrostatic actuation system commanded by the DRS into voltages to be commanded to the ISS.

In the period in question, only 15 anomalies were detected that caused the FDIR to go to the LTP safe condition, either by switching back to ACC3 or by applying the emergency grab operation on both test masses and going to pure SC attitude control. All anomalies could be traced back to some hardware issue (e.g., DRS thruster failure) or an external event like a micrometeorite strike. Nevertheless, in all cases, the FDIR worked as expected and the SC was able to resume science operations shortly after.

6 Conclusions and lessons learned

From switch on to extended mission operation, the LISA Pathfinder drag-free and attitude control system has worked flawlessly with performances far below the requirements. The mission has demonstrated the readiness of the technology for application in a gravitational wave observatory like LISA. The success has been made possible by a deep understanding of the LTP system that has been acquired during the LISA Pathfinder DFACS development and implementation phase. Close cooperation with the instrument engineering team is considered of major importance also for a future gravitational wave observatory like LISA. The heritage in system understanding gained by Airbus Friedrichshafen is considered as major risk mitigation for the design of the LISA drag-free and attitude control system.

The release process has to be improved in terms of release conditions. An evolution of the control algorithms based on the LPF design is proposed to further increase the acceptable release velocities which also would ease ground verification of the mechanism. Nevertheless, the sliding mode implementation of the accelerometer mode has proven to be the right choice to provide a robust control system to cope with the large uncertainties in the release conditions.

References

1. Racca, G., et al.: The LISA Pathfinder mission. Space Sci. Rev. **151**, 159–181 (2010)
2. Danzmann, K., et al.: LISA: Unveiling a hidden Universe. Report No. ESA/SRE2011(2011)3 (2011)
3. Brandt, N., et al.: LISA Pathfinder Experiment Performance Budget, S2-ASD-RP-3036, Issue 3 (2015)
4. Armano, M., et al.: Sub-Femto-g free fall for space-based gravitational wave observatories: LISA Pathfinder results. PRL **116**, 231101 (2016)
5. Fichter, W., et al.: Control tasks and functional architecture of the LISA Pathfinder drag-free system. In: Danesy, D. (ed.) Proceedings of the 6th ESA Conference on Guidance, Navigation, and Control Systems, vol. SP-606, ESA Publications Division (2006)
6. Fichter, W., et. al.: Closed loop performance and limitations of the LISA Pathfinder drag-free control system. In: Proceedings of the AIAA guidance, navigation and control conference, AIAA 2007-6732, Hilton Head, South Carolina, 20–23 Aug 2007 (2007)
7. Fichter, W., et al.: Drag-free control design with cubic test masses, lasers, clocks and drag-free. In: Dittus, H., Laemmerzahl, C., Turyshev, S. (eds.) pp. 365–380. Springer, Berlin (2007)
8. Slotine, J.J., et al.: Applied Nonlinear Control. Prentice-Hall International Inc, Upper Saddle River (1991)
9. Vitale, S.: The LTP experiment on LISA Pathfinder and its first results, LISA Symposium 2016, University of Zurich, Switzerland, 5–9 (2016)